Talanta 217 (2020) 121117

Contents lists available at ScienceDirect

Talanta

journal homepage: www.elsevier.com/locate/talanta

Phosphoglycan-sensitized platform for specific detection of anti-glycan IgG and IgM antibodies in serum

Danilo Echeverri[a], Monika Garg[b], Daniel Varón Silva[b], Jahir Orozco[a,*]

[a] Max Planck Tandem Group in Nanobioengineering, University of Antioquia, Complejo Ruta N, Calle 67 N° 52–20, Medellín, 050010, Colombia
[b] Department of Biomolecular Systems, Max Planck Institute of Colloids and Interfaces, Am Mühlenberg 1, 14476, Potsdam, Germany

ARTICLE INFO

Keywords:
Glycobiosensor
Glycosylphosphatidylinositol
Label-free
T. gondii
IgG

ABSTRACT

Glycosylphosphatidylinositol anchored proteins (GPI-APs) are natural conjugates in the plasma membrane of eukaryotic cells that result from the attachment of a glycolipid to the C-terminus of many proteins. GPI-APs play a crucial role in cell signaling and adhesion and have implications in health and diseases. GPI-APs and GPIs without protein (free GPIs) are found in abundance on the surface of the protozoan parasite *Toxoplasma gondii*. The detection of anti-GPI IgG and IgM antibodies allows differentiation between toxoplasmosis patients and healthy individuals using serological assays. However, these methods are limited by their poor efficiency, cross-reactivity and need for sophisticated laboratory equipment and qualified personnel. Here, we established a label-free electrochemical glycobiosensor for the detection of anti-GPI IgG and IgM antibodies in serum from toxoplasmosis seropositive patients. This biosensor uses a synthetic GPI phosphoglycan bioreceptor immobilized on screen-printed gold electrodes through a linear alkane thiol phosphodiester. The antigen-antibody interaction was detected and quantified by electrochemical impedance spectroscopy (EIS). The resultant device showed a linear dynamic range of anti-GPI antibodies in serum ranging from 1.0 to 10.0 IU mL^{-1}, with a limit of detection of 0.31 IU mL^{-1}. This method also holds great potential for the detection of IgG antibodies related to other multiple medical conditions characterized by overexpression of antibodies.

1. Introduction

Many proteins of eukaryotic cells are tethered to the plasma membrane via a glycosylphosphatidylinositol glycolipid (GPI) attached to the C-terminus of the proteins, forming the so-called GPI-anchored proteins (GPI-APs) [1]. GPI-APs play a crucial role in cell communication, signaling and adhesion and act as immunomodulators during infectious diseases. GPI-APs and GPIs without protein (free GPIs) are found in abundance on the surface of the protozoan *Trypanosoma brucei, Plasmodium falciparum, Toxoplasma gondii* [2], and *Trypanosome cruzi* [3]. Protozoan GPIs modulate the host immune system and elicit an early anti-GPI antibody (IgG and IgM) response in human infection by *T. gondii* [4,5]. Recently, a synthetic GPI phosphoglycan printed on microarrays was used for the detection of anti-GPI IgG and IgM antibodies in serum. This test allowed a distinction of *T. gondii* seropositive from healthy individuals and differentiation between sera from patients having an acute or a latent stage of the infection [6,7]. In this context, antibody levels in serum correlate well with host-pathogen interactions and the development of infectious diseases [8,9], as well as with the development of other more complex diseases, such as inflammatory responses and cancer [10–14].

The Enzyme-Linked Immunosorbent Assay (ELISA) is the gold standard method to determine antibody levels in serum and for the diagnosis of a variety of infectious diseases, including Toxoplasmosis [15–17]. Other commonly used methods to detect antibodies against *T.gondii* antigens are the Indirect Fluorescent Antibody Test assay (IFAT), Indirect hemagglutination test (IHA), Immunosorbent agglutination assay (ISAGA) and Western Blotting (WB) [18]. However, these methods have some limitations, including reduced efficiency, cross-reactivity, and the need for sophisticated laboratory equipment, and qualified personnel [19,20]. Therefore, cost-efficient and rapid tests with high accuracy, specificity and sensitivity must be implemented for the timely diagnosis of multiple diseases [21].

Electrochemical biosensors offer a valuable alternative for biomarkers detection with high specificity, sensitivity, low cost and the possibility of implementation at the point-of-care [22]. Biosensors have been developed for the detection of multiple pathogens using a myriad of bioreceptors, such as antibodies, nucleic acids, aptamers and peptides, among others [23–26]. However, the use of glycans as bioreceptors in biosensor platforms is less explored despite their potential

* Corresponding author.
E-mail address: Grupotandem.nanobioe@udea.edu.co (J. Orozco).

https://doi.org/10.1016/j.talanta.2020.121117
Received 3 February 2020; Received in revised form 29 April 2020; Accepted 1 May 2020
Available online 04 May 2020
0039-9140/

application for the development of new diagnostic tests [6,7].

Biosensing based on electrochemical impedance spectroscopy (EIS) is sensitive, allows detection of analytes at low concentrations, and does not require labeling to follow the biorecognition event [27–29]. The EIS requires a pair-redox solution and a sinusoidal potential with a small amplitude over a broad frequency range to determine the quantitative parameters of the electrochemical processes that are taking place. Parameters are estimated by using a Randles-type equivalent circuit, which explains both bulk and interfacial electrical properties of the system, by fitting the experimental data [29,30]. In the development of an impedimetric biosensor, the bioreceptors that bind specifically to the target molecules are immobilized on the working electrode surface. If the biorecognition event occurs on the functionalized surface, the analyte molecules bound to the bioreceptor change the interfacial properties in an analyte concentration-dependent manner [27,30].

Here, we report a simple label-free electrochemical biosensor for monitoring anti-glycan IgG antibodies in serum from toxoplasmosis seropositive patients. The biosensor uses a synthetic GPI phosphoglycan bioreceptor immobilized on screen-printed gold electrodes (SPAuEs) through a linear alkane thiol phosphodiester. The antigen-antibody interaction was detected and quantified by electrochemical impedance spectroscopy (EIS). The resultant device showed a linear dynamic range of anti-GPI antibodies in serum ranging from 1.0 to 10.0 IU mL^{-1}, with a limit of detection of 0.31 IU mL^{-1} and less than 4% of deviation with respect to quantification by IFAT assay. The glycobiosensor was specific for *T. gondii*, detecting and quantifying anti-GPI antibodies from toxoplasmosis seropositive patients. This method allows for the detection of Toxoplasmosis and offers considerable potential for quantification of anti-glycan antibodies using other biomarkers and the development of other glycan-based diagnostic tests closer to the patient.

2. Materials and methods

2.1. Reagents and solutions

Tris(2-carboxyethyl) phosphine hydrochloride (TCEP), bovine serum albumin (BSA), potassium ferricyanide ($K_3[Fe(CN)_6]$) and potassium ferrocyanide ($K_4[Fe(CN)_6]\cdot 3H_2O$) were purchased from Merck Millipore. Tween-20 and disodium hydrogen phosphate (Na_2HPO_4) were acquired from Panreac AppliChem. Potassium dihydrogen phosphate (KH_2PO_4), potassium chloride (KCl) and sodium chloride (NaCl), were purchased from J. T Baker. Sulphuric acid (H_2SO_4) was acquired from Fluka TM. All reagents were used as received and the solutions were prepared using deionized water of 18 MΩ cm from a Smart2Pure 3 UV/UF Milli-Q system. Phosphate Buffered Saline (PBS, 1X, pH 7.4) was used to prepare the bioreceptor solution and serum samples.

2.2. Preparation of the synthetic GPI solution

The phosphoglycan from the free GPI of *T. gondii,* also called as low molecular weight antigen, was synthesized containing a thiol-linker by a convergent strategy following previously reported protocols [7,31,32]. 100 μg of the GPI phosphoglycan (MW: 1470 g mol^{-1}) were dissolved in 340 μL of PBS to prepare a 200 μM glycan stock solution. TCEP was added at a final concentration of 200 μM to reduce thiol groups from the GPI that may be oxidized.

2.3. Equipment and pretreatment of SPAuEs

All the electrochemical measurements were performed in a potentiostat/galvanostat VersaSTAT 3 and the EIS Spectrum Analyser software was used for EIS analysis. SPAuEs were purchased from DropSens (ref. 250 BT). They consist of a 4 mm working electrode, a platinum counter electrode, and a silver pseudo-reference electrode, respectively arranged all together in a ceramic substrate.

SPAuEs were electrochemically activated in 0.1 M H_2SO_4 by using Cyclic Voltammetry (CV) in a potential window between +1.6 V and 0 V (*vs* Ag pseudo-reference electrode) at a scan rate of 0.1 Vs^{-1} until the CV becomes stable (approximately 12 cycles). The effective area was estimated by taking into account that the reductive peak from the gold surface has a charge of 400 μC cm^{-2} [33,34]. The electroactive area (*A*) of the electrodes was calculated from the CV experiments in 1 mM $K_3[Fe(CN)_6]$/0.1 M KNO_3, at 50 mV/s by using the Randles-Sevcik equation [35].

2.4. Quantification of IgG antibody by IFAT assay

Serum samples from healthy individuals (non-reactive for *T. gondii*) and patients diagnosed with Toxoplasmosis were kindly provided with the corresponding antibody titers by the biobank of the Parasitology Group from the Faculty of Medicine at the University of Antioquia (Medellín-Colombia). The antibody concentrations (250, 500 and 1000 IU mL^{-1}) were quantified by IFAT assay [36]. This methodology is briefly described as follows. Trophozoites of *T. gondii* were propagated in mice peritoneum and then harvested 3–4 days post-inoculation. Next, trophozoites were fixed on a glass slide and incubated with different test serum dilutions. An anti-IgG antibody labeled with fluorescein isothiocyanate (anti-human IgG/FITC) was added and left to react with the antibodies attached to the surface of the trophozoites cellular membrane. The labeled samples were observed under a fluorescence microscope. The antibody concentration was determined by comparing with serial dilutions of a commercial IgG positive control of 200 IU mL^{-1} (Toxotrol-F, bioMérieux, Ref. 75411).

2.5. Preparation of test serum samples and assembling of the biosensor

All experiments were performed in triplicate for each condition. The gold working electrode from the SPAuEs was functionalized with the GPI phosphoglycan by chemisorption of the thiol-linker attached to the *myo*-inositol. The functionalization was achieved by adding 4 μL of the GPI glycan stock solution on the gold working electrode and incubated for 1 h at room temperature in a humid chamber. Different concentrations of glycan (50, 100 and 200 μM) were evaluated to obtain the optimal conditions based on the highest signal/noise ratio. The phosphoglycan solution was either drop cast on the SPAuE or diluted in a 1X PBS pH 7.4 solution down to the final concentration of 50 and 100 μM, as appropriate. The electrode was washed twice with PBS and deionized water to remove unbound glycan molecules. Finally, the nonspecific binding sites of the electrode were blocked by incubation with 5 μL of 1% BSA solution for 30 min at room temperature in the humid chamber. BSA and GPI (estimated by the Glycan Reader & Modeler and the Glycolipid modeler) [37] have a size of the same order of magnitude, and similar to observations in previous reports [38,39]. We expect the phosphoglycan to remain accessible for binding to antibodies.

The sera were diluted 1:100 with PBS containing 0.1% Tween-20 (v/v) and 3% BSA (w/v). They were then pretreated by vortexing for 15 s and incubated at 37 °C for 15 min to dissolve the possible lipid aggregates that may be present in the matrix. The insoluble residual components of the sample were removed by centrifugation at 13000 rpm for 5 min. 5 μL of pretreated serum samples were dropped cast onto the modified working electrode and incubated in the humidity chamber for 15 min at 37 °C to bind anti-GPI antibodies. Finally, a series of washing steps with PBS 1X pH 7.4 and deionized water were performed to remove the antibodies that did not bind to the GPI-bioreceptor.

2.6. Electrochemical measurements

The electrochemical performance of the as-functionalized platform was evaluated by CV by using the redox pair 5 mM $[Fe(CN)_6]^{3-/4-}$/PBS 1X, pH 7.4 in a potential window between +0.5 V and −0.1 V, at a

scanning rate of 0.05 Vs^{-1} for 5 consecutive cycles. This measurement was made initially with the bare electrode and later after each step of the functionalization process.

EIS measurements were carried out in the presence of the redox pair 5 mM $[Fe(CN)_6]^{3-/4-}$/PBS 1X, pH 7.4, by applying a potential of +0.18 V with an amplitude of 10 mV and frequencies ranging from 50 kHz to 0.01 Hz. The impedance measurements were performed after modifying the surface of the SPAuE with the GPI-glycan by chemisorption and after each step of the biosensor development, *i.e.* functionalization of the electrodes with the GPI, blocking the electrodes with BSA; and incubation with seronegative and seropositive serum samples.

Different serum dilutions with known IgG antibody concentrations (titers measured by the IFAT assay) were evaluated by EIS using the difference in charge transfer resistance (ΔR_{ct}) as the response variable for quantification and building the biosensor calibration curve. Changes in resistance were calculated according to $\Delta R_{ct} = R_{ct}$ (GPI-BSA-Ab) - R_{ct} (GPI-BSA), where R_{ct} (GPI-BSA) is the value of the charge transfer resistance having the GPI and BSA immobilized on the electrode and R_{ct} (GPI-BSA-Ab) is the resistance value after the interaction with the serum [40]. Proper volumes of 1000 IU mL^{-1} of reactive serum were diluted up to 1 mL of buffer to get 1.0, 2.5, 5.0, 7.5 and 10 IU mL^{-1} and the resultant solutions were pretreated as mentioned in the 2.5 section. The limit of detection (LOD) and the limit of quantification (LOQ) of the biosensor were determined by using the 3-sigma and 10-sigma criteria, respectively [41], with LOD = $3S_b/m$ and LOQ = $10S_b/m$, where S_b is the standard deviation for the signal obtained from non-reactive serum and m is the slope of the calibration curve.

2.7. Quantification of antibodies in human serum and specificity studies

As proof of concept, the concentration of antibodies in serum from patients diagnosed with toxoplasmosis was quantified. Three different serum samples with antibody titers of 250, 500 and 1000 IU mL^{-1} diluted and pretreated as in section 2.5 were evaluated. These titers were measured by using the IFAT assay, as mentioned above.

To assess the specificity of the anti-GPI antibodies detection for toxoplasmosis, we evaluated the cross-reactivity of the GPI-based glycobiosensor to antibodies in serum from seropositive patients for *P. falciparum* and *T. cruzi* infections. This analysis was completed by using the protocols for the detection of antibodies in the *T. gondii* seropositive samples and EIS to follow the interaction. To evaluate the statistical significance between the samples, a paired *t*-test and a 1-way ANOVA with a level of statistical significance of 99% (ANOVA) was performed, using the Excel software.

3. Results and discussion

3.1. Development of the detection system

We selected the phosphoglycan of the free GPI of *T. gondii* as a biomarker for the development of a biosensor to detect anti-glycan antibodies in serum. The structure of this phosphoglycan consists of the GPI core, (a lipid, a phospho-myo-inositol (Ino), a glucosamine (GlcN), three mannoses (Man) and a phosphoethanolamine (PEtN) forming the EtNP-6Man-α-(1 → 2)-Man-α-(1 → 6)-Man-α-(1 → 4)-GlcN-α-(1 → 6)-Ino-phospholipid glycolipid), having an α-Glc-(1 → 4)-β-GalNAc side branch at the O4-position of the first mannose, Fig. 1 [1,2,42,43]. The α-Glc unit presents in the side branch is highly immunogenic and triggers an immunoglobulin (IgM) antibody response in human infection with *T. gondii* [5,7,44]. Instead of the naturally attached phospholipid attached to the myo-inositol unit, the GPI was modified with a phosphodiester having a thiol-alkyl linker. This modification ensures the GPI regio- and chemo-selective immobilization on a solid support preserving the amine groups of the GPI intact and available to interact with the antibodies [7,45].

We started the glycobiosensor development with the chemisorption of the phosphoglycan on the SPAuE surface (Fig. 1, left side). To obtain an efficient, reproducible and controlled formation of a self-assembled monolayer of the GPI on the SPAuE [46], the surface of the SPAuE was first activated by CV in acidic conditions. The resultant effective area was estimated by using a gold surface charge of 400 μC cm^{-2}. The effective area (A_e = 305.0 ± 2.9 mm^2) was compared with the geometric area of the working electrode reported by the manufacturer (A_g = 12.6 mm^2) and the surface roughness factor (A_e/A_g) was maintained at 24.2 ± 0.2 to ensure a constant A_e in each SPAuE. An electroactive area (A) of 12.5 ± 0.05 mm^2 was calculated from the CV experiments in 1 mM $K_3[Fe(CN)_6]$/0.1 M KNO_3, at 50 mV/s by using the Randles-Sevcik equation, which corresponded to 99% of A_g. This result indicated the proper activation of the electrode surface [47] with an interelectrode relative standard deviation lower than 3% (n = 10) in all cases. The effective area involves the surface roughness and heterogeneous points, energetically different, where current may pass through depending on the phase boundary. The electrochemical area accounts for the area available for the oxidation and reduction of the electrochemical probe [48,49].

The activated gold working electrode was successively treated with the phosphoglycan and BSA and was characterized by CV and EIS. Only small changes of the electrochemical behavior (CVs) and slightly lower current intensity were observed after the SPAuE modification with a 200 μM solution the GPI, after the blocking with 1% BSA and after the incubation of the modified electrode with a non-reactive serum or with a reactive serum having 10 IU mL^{-1} concentration (Fig. 2A). However, changes in the electrochemical behavior were more evident using EIS, which showed an increase in the charge transfer resistance after each modification step (Fig. 2B).

The changes in the electrical properties are evidence of biomolecules' immobilization on the working electrode surface, thereby hindering the conduction of electrons from the bulk solution to the electrode surface. The electrochemical process is represented by the equivalent circuit depicted in Fig. 2B (inset), where R_s is the electrolyte solution resistance, R_{ct} is the charge transfer resistance and *CPE* is the constant phase element. *CPE* depends on a pre-exponential factor (P) and an exponent (n). It is used herein instead of the typical double-layer capacitance to take into account the interfacial heterogeneity of the electrode surface [50]. P values indicated a decrease in the capacitive behavior of the system, and n values for modified electrodes were less that one, consistent with a pseudo interfacial double layer capacitance at the electrode/electrolyte interface [51]. R_{ct} was estimated from the semicircle of the impedance spectra in the high-frequency region, which corresponds to the limited electron transfer process that indicates the electrode surface is blocking the electrons flow from the redox probe. We used the R_{ct} signal to follow the bioreceptor-analyte interaction [52].

The EIS from the bare electrode in Fig. 2B shows that the semicircle diameter in the Nyquist plot is very similar to the charge transfer resistance, R_{ct} = 131 ± 28 Ω, because the R_s = 22 ± 0.3 Ω is very low [53]. In contrast, R_{ct} increased considerably (up to 4870 ± 446 Ω) after the phosphoglycan immobilization on the electrode due to an increase in the interface thickness that insulated the conductive support and blocked the interfacial electron transfer. This change also indicates the successful absorption of the phosphoglycan on the electrode [54]. The blocking of the non-specific adsorption sites on the SPAuE with BSA induced a slightly additional increase in the insulation and R_{ct} value (Fig. 2B).

We evaluated the effect of the interaction of the modified electrode with a seronegative and seropositive serum for toxoplasmosis in its electrochemical parameters. When the GPI-electrode was incubated with the non-reactive serum, there was no significant increase in the R_{ct} value, consistent with the lack of recognition event. However, when the GPI-electrode was incubated with the reactive serum, a glycan-antibody binding induced an increase of the R_{ct} to a value of 11778 ± 483 Ω.

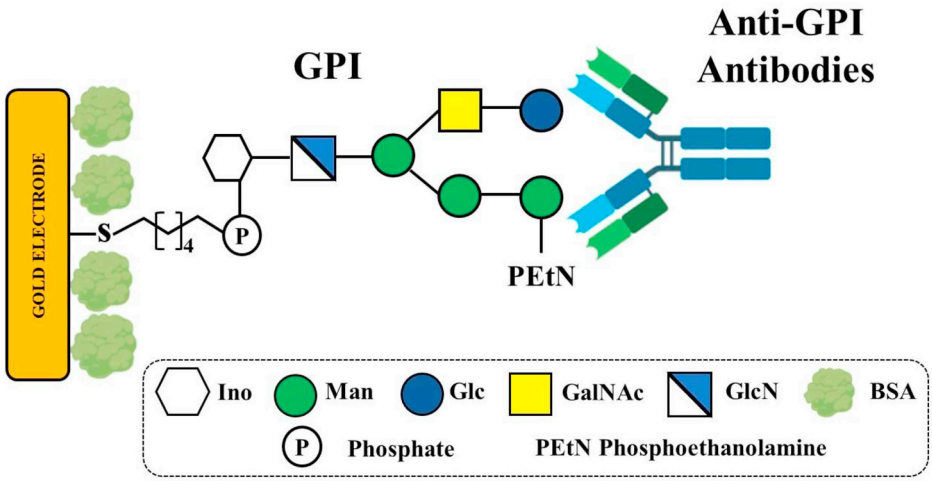

Fig. 1. Schematic representation of the functional platform development.

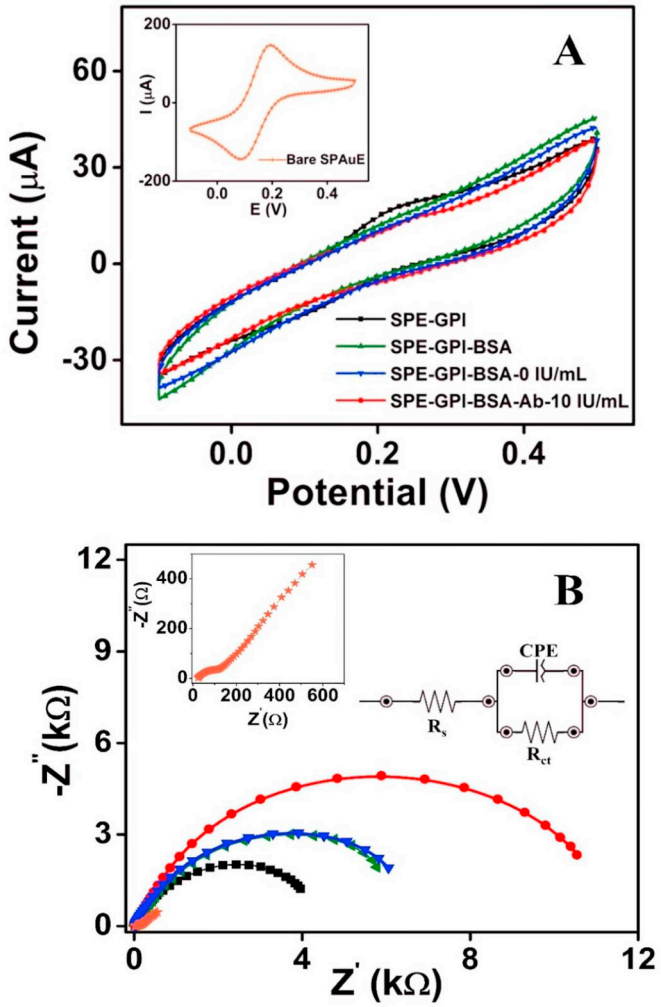

Fig. 2. A) Cyclic voltammograms for each modification step at a scan rate of 50 mV/s (the bare electrode is in the inset), **B)** Nyquist plot with frequency range 50 kHz to 0.01 Hz, amplitude 10 mV (the bare electrode and the equivalent Randles circuit are in the inset). The redox probe is 5 mM $[Fe(CN)_6]^{3-/4-}$/PBS 1X, pH 7.4.

The very small values of Chi-squared function (χ^2) for the best-fitted equivalent circuit, lower than 1.5×10^{-2}, demonstrated that the curve showed herein (the raw values) and the experimental data from the mathematical fitting agreed (S.I. Figure S1). Therefore, EIS results will show only raw data from now on. Table 1 summarizes all the fitted electrochemical parameters.

3.2. Optimization of GPI concentration

Once the functionality of the biosensor platform was established, the glycan concentration was optimized based on the best signal/noise ratio to differentiate binding of antibodies to the glycan, in a reactive serum with 10 IU mL^{-1} with respect to a non-reactive serum (0 IU mL^{-1}) (Fig. 3). The behavior of the electrode functionalized with different concentrations of the glycan was evaluated after BSA blocking and incubation with the serum. The best signal-to-noise ratio (S/N = 1.6) and a bigger ΔR_{ct} was obtained by chemisorption of the bioreceptor at 200 μM; therefore, this concentration was selected for the next experiments (building of the calibration curve). At this concentration, a higher amount of glycan should be immobilized on the electrode surface and be available for interaction with the antibodies in the sera. Furthermore, a high glycan density may enhance the blocking of the surface and decrease the nonspecific adsorption of proteins.

3.3. Analytical parameters and calibration curve

Having an optimal glycan concentration, we evaluated the glycobiosensor analytical performance by analyzing different dilutions from the 1000 IU mL^{-1} reactive serum solution, containing final concentrations of antibodies ranging from 1.0 to 10.0 IU mL^{-1} and pretreated as detailed in the materials and methods section. We built a calibration curve by estimating the ΔR_{ct} for each antibody concentration solution (Fig. 4). The data showed a linear correlation described by the equation ΔR_{ct} = 475*[Ab] + 106 and a correlation coefficient R^2 = 0.999 (Fig. 4B). The LOD was estimated to be 0.31 IU mL^{-1} and the LOQ 1.00 IU mL^{-1}. After considering the 100-fold serum dilution factor from the pretreatment and taking into account that levels of IgG in serum > 300 IU mL^{-1} suggests a recent infection [55], our results indicate that the glycan-based biosensor is able to detect clinically relevant antibody concentrations. In this context, the device can be used not only for the serological diagnosis of toxoplasmosis in the active stage of the infection but can detect seropositive status with a cut-off index > 30 IU mL^{-1} [56]. Besides, it has been reported that IgG serum levels in healthy individuals can be in the range of 91–118 IU mL^{-1} [57], which can be detected by our biosensor. Furthermore, the sensitivity of the biosensor could be further enhanced by implementing an amplification strategy such as an enzyme-labeled secondary antibody [58,59] or by immobilizing the GPI onto a modified nanomaterial of larger surface, thereby enhancing its electrochemical properties and

Table 1
Electrochemical characterization of the modified electrodes. Data from EIS experiments. Charge-transfer resistance (R_{ct}), electrolytic solution resistance (R_s), constant phase element (*CPE*) with pre-exponential factor (*P*) and exponent (*n*) and Chi-squared function (χ^2).

SPAuE	R_{ct} (kΩ)	R_s (Ω)	CPE		χ^2
			P (F)	n	
GPI	4.87 ± 0.446	24.8 ± 1.06	1.11×10^{-4}	0.806	5.80×10^{-3}
GPI/BSA	7.48 ± 0.339	22.5 ± 0.650	9.07×10^{-5}	0.813	5.47×10^{-3}
GPI/BSA/0 IU mL^{-1}	7.53 ± 0.585	23.1 ± 1.21	5.82×10^{-5}	0.840	2.38×10^{-3}
GPI/BSA/10[a] IU mL^{-1}	11.8 ± 0.483	23.7 ± 0.944	6.02×10^{-5}	0.867	1.48×10^{-2}

[a] Concentration obtained from a dilution 1:100 from the stock.

increasing its analytical performance [60,61].

3.4. Biosensor specificity, repeatability and reproducibility

The specificity of the glycobiosensor is essential to reduce or avoid a false positive assignment. We considered herein the cross-reactivity of the phosphoglycan to *T. gondii* with respect to antibodies in serum from people who were positive for malaria and Chagas' disease by the Polymerase Chain Reaction (PCR) gold standard method. These infections are caused by the protozoa *P. falciparum* and *T. cruzi* that have high amounts of GPIs on their cell surface. These GPIs lack the galactosamine-glucose side branch, but they also induce the production of anti-GPI antibodies that may interact with the synthetic GPI phosphoglycan from *T. gondii* used as bioreceptor. The Nyquist plot from the EIS measurements shows that the corresponding ΔR_{ct} was higher for the reactive serum-containing antibodies against *T. gondii* GPI (ΔR_{ct} = 4864 ± 29 Ω) compared to those that may contain antibodies against *P. falciparum* (ΔR_{ct} = 996 ± 231 Ω) and *T. cruzi* (ΔR_{ct} = 1274 ± 238 Ω) GPIs, corresponding to concentrations of 1001, 190 and 250 IU mL^{-1}, respectively (Fig. 5A). The resultant EIS signals exhibited a differential response with significant statistical differences when analyzed by a paired *t*-test and a 1-way ANOVA with a level of statistical significance of 99%. Yet, the slight cross-reactivity indicates a slight interaction of the phosphoglycan from *T. gondii* with antibodies against *P. falciparum* and *T. cruzi,* which could be explained by the immunodominant role of GPI glycolipids and the structural similarities between all GPIs. Furthermore, high levels of IgG anti-GPI have been associated with an increased risk of malaria, thus suggesting that they are biomarkers of increased exposure to *P. falciparum* infections [62]. Similarly, during infection with *T. cruzi*, GPIs activates the innate and adaptive immune responses, resulting in the production of IgG antibodies [63]. The results suggest that our device can detect anti-GPI antibody concentrations higher than 31 IU mL^{-1}, which will cover most of the seropositive sample from acute infections, and it is in agreement with the determination of seropositive sera using other tests [56,64]. Higher levels can be considered reactive and lower levels can be either indeterminate or non-reactive [56]. Further optimization of the assay is necessary to reduce the LOD of the glycobiosensor and cover samples with lower antibody concentrations. In further applications, the observations mentioned above should be considered to use the detection of antibodies and determine the presence of an infection.

We evaluated the repeatability and inter-electrode reproducibility of our device by measuring the response of freshly prepared electrodes with 200 μM GPI - 1% BSA to 10 IU mL^{-1} of antibody concentration. These values were compared to the response of electrodes in non-reactive serum (0 IU mL^{-1}) and used to estimate the *ΔRct*. The

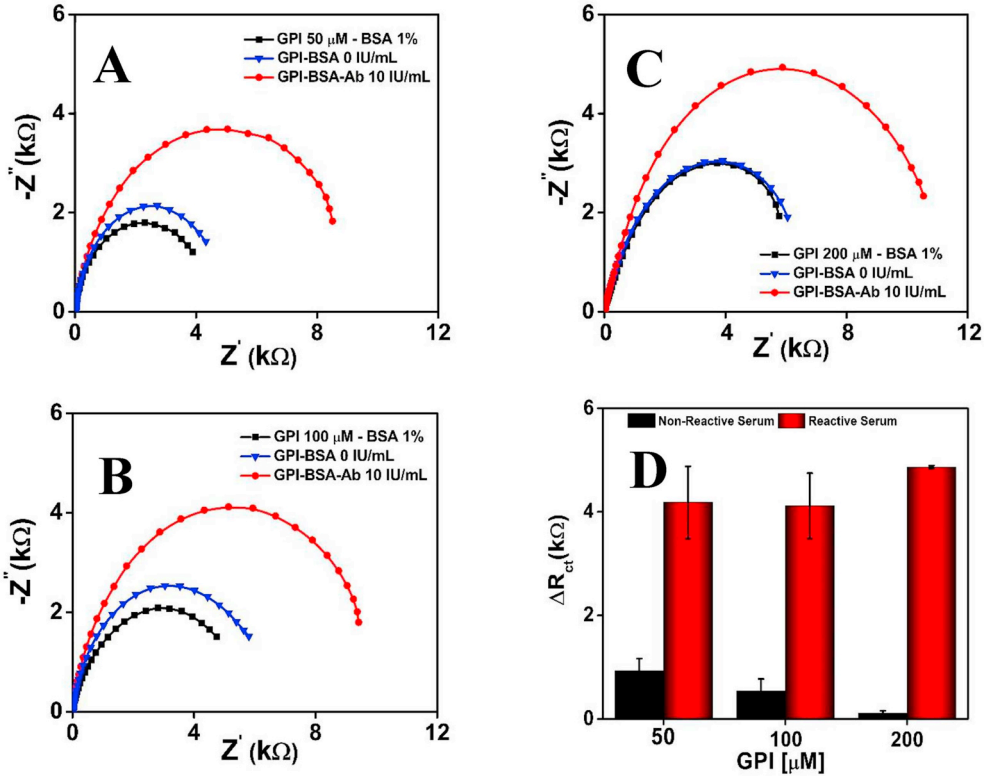

Fig. 3. Nyquist plots recorded using the redox probe 5 mM $[Fe(CN)_6]^{3-/4-}$/PBS 1X, pH 7.4. Frequency from 50 kHz to 0.01Hz and amplitude 10 mV. [GPI]: **(A)** 50 μM, **(B)** 100 μM and **(C)** 200 μM. **(D)** The difference in the charge transfer resistance of reactive and non-reactive serum for the different concentrations of GPI bioreceptor.

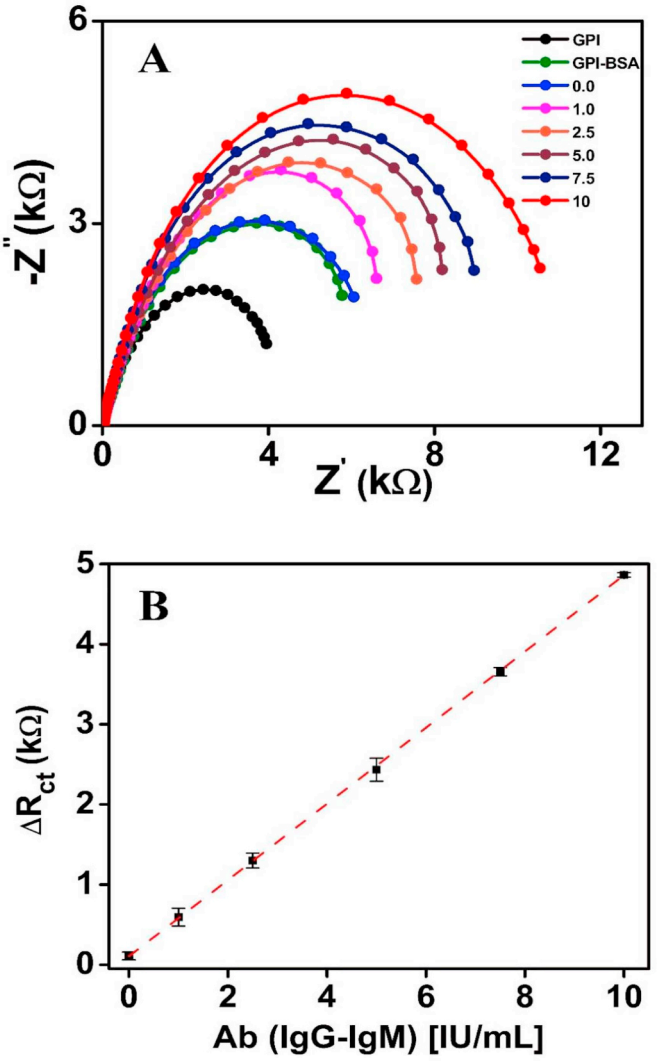

Fig. 4. (A) Nyquist plots for different antibody concentrations (IU mL^{-1}) with 5 mM $[Fe(CN)_6]^{3-/4-}$/PBS 1X, pH 7.4 as redox probe, frequency range from 50 kHz to 0.01Hz and amplitude 10 mV; and **(B)** Resultant calibration curve, with the difference in charge transfer resistance as a response variable.

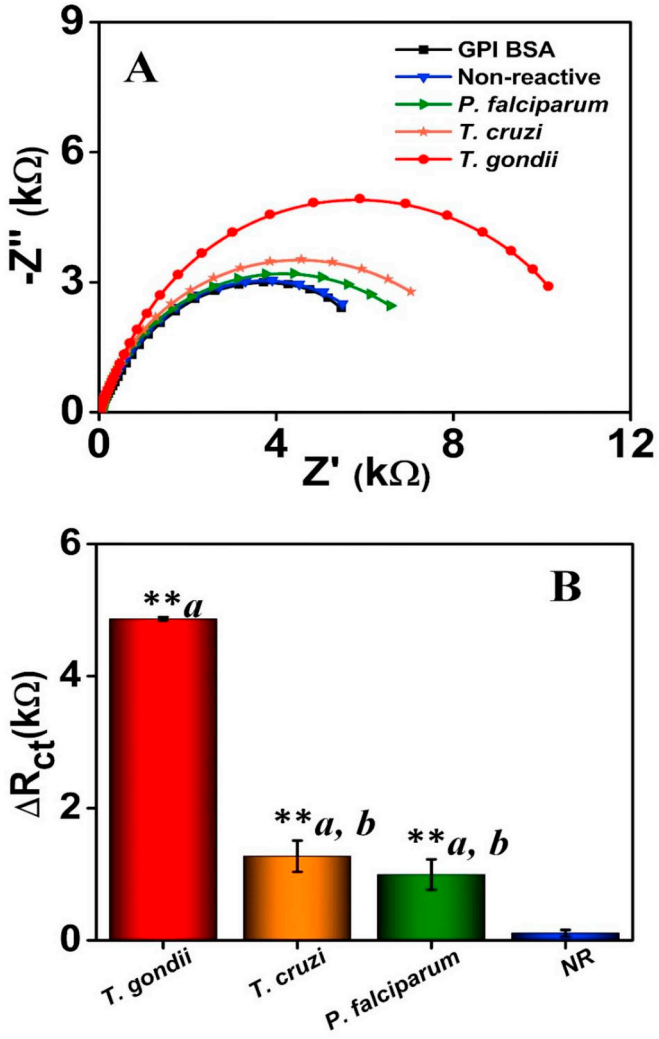

Fig. 5. (A) Nyquist plots of reactive serum samples for *P. falciparum*, *T. cruzi* and *T. gondii* and non-reactive serum (NR) with 5 mM $[Fe(CN)_6]^{3-/4-}$/PBS 1X, pH 7.4 as redox probe, frequency range from 50 kHz to 0.01Hz, amplitude 10 mV. **(B)** The difference in the charge transfer resistance for each serum sample. (****a**) Significantly different respect to the non-reactive serum ($p < 0.01$). (****b**) Significantly different respect to the *T. gondii* reactive serum ($p < 0.01$).

repeatability and inter-electrode reproducibility were estimated to be 2.41% (n = 3) and 3.27% (n = 4), respectively. Different strategies have been reported to regenerate the gold electrode surface [33,65]. However, we did not reuse the SPAuE to avoid changes of the electrical properties at the transducer surface that may be detected by the highly sensitive EIS over regeneration cycles [65]. Therefore, all measurements use fresh-prepared sensitized surfaces.

3.5. Quantification of antibodies in human serum

To test the potential of the developed glycobiosensor for the determination of toxoplasmosis serostatus, we compared the response of the biosensor in toxoplasmosis seropositive samples with different antibodies titers determined by the IFAT assay. The antibody concentration was calculated by extrapolation of the ΔR_{ct} values obtained for each serum sample in the calibration curve depicted in Fig. 4B. A correlation of the concentration of antibodies in human serum determined by EIS showed a relative error lower than 4% with respect to the IFAT method (Table 2). Furthermore, the ANOVA test suggests that there are no significant differences comparing the two methods ($p > 0.01$). It is important to remark that whereas the IFAT assay measures the anti-IgG anti-toxoplasma antibody concentration, the glycobiosensor measures a mix of IgG and IgM antibodies instead; therefore an overestimation of the concentration of IgG may be related to IgMs.

Table 2
Antibody measurements in human serum using the electrochemical biosensor and the corresponding error concerning the measurement from the standard IFAT method.

[IgG and IgM] by EIS (ΔR_{ct} (kΩ))	[IgG] by IFAT	Relative Error (%)
260 IU mL^{-1} (1.34 ± 0.093)	250 IU mL^{-1}	4.0
520 IU mL^{-1} (2.59 ± 0.145)	500 IU mL^{-1}	4.0
1014 IU mL^{-1} (4.93 ± 0.231)	1000 IU mL^{-1}	1.4

The serum antibody levels quantified with the electrochemical glycobiosensor correlate well with the seropositive diagnosis, thus allowing for differentiation between healthy individuals and infected patients. Furthermore, results demonstrated the glycan structure specifically recognized all reactive serum that showed high levels of IgG antibodies, in agreement with Götze et al. In contrast, results from the non-reactive serum samples correlated well with low levels of these antibodies [7].

4. Conclusions

We developed a glycobiosensor that allows the detection and quantification of IgG and IgM anti-GPI antibodies, which are biomarkers currently used for the diagnosis of diseases. The sensing platform uses a synthetic GPI from *T. gondii* that recognized serum antibodies and lead to differentiation between healthy individuals and patients diagnosed with toxoplasmosis. The phosphoglycan has been reported as a specific antigen for toxoplasmosis diagnosis in a microarray- and bead-based format. The electrochemical method reported herein offers new opportunities for diagnosis in decentralized settings. The high performance of the glycobiosensor allowed us to detect a concentration of antibodies of clinical relevance in serum samples and determine positive serostatus reactive against *T. gondii*. An augmented glycobiosensor response was related to an increase of toxoplasma antibodies, thus demonstrating that our method would be suitable for the diagnosis of acute toxoplasmosis. Overall, the quantification of IgG and IgM antibodies in serum samples and the discrimination of toxoplasmosis infectious were demonstrated by the label-free EIS method. However, the glycobiosensor offers also opportunities for diagnosis of multiple medical conditions that are based on antibody detection.

CRediT authorship contribution statement

Danilo Echeverri: Methodology, Writing - original draft, Investigation, Data curation, Formal analysis. **Monika Garg:** Methodology. **Daniel Varón Silva:** Formal analysis, Writing - review & editing. **Jahir Orozco:** Formal analysis, Funding acquisition, Project administration, Conceptualization, Writing - original draft, Supervision.

Declaration of competing interest

The authors declare there is no conflict of interest.

Acknowledgments

The work has been funded by COLCIENCIAS, through the Program *Ecosistema Científico* Cod. FP44842-211-2018 (Project number, 58536). J.O thanks support from The University of Antioquia and the Max Planck Society through the cooperation agreement 566-1, 2014. MG and DVS thank the Max Planck Society and the RIKEN Max Planck Joint Center for Systems Chemical Biology for the financial Support. We thank the Parasitology Group from the Faculty of Medicine and Dr Carlos Muskus from PECET, at Universidad de Antioquia (Medellín-Colombia) for providing us the *T. gondii* reactive and nonreactive serum samples and with *T. cruzi,* and *P. falciparum* reactive serum samples, respectively. We thank The Ruta N complex for hosting the Max Planck Tandem Groups.

Appendix A. Supplementary data

Supplementary data to this article can be found online at https://doi.org/10.1016/j.talanta.2020.121117.

References

[1] S. Saha, A.A. Anilkumar, S. Mayor, GPI-anchored protein organization and dynamics at the cell surface, J. Lipid Res. 57 (2016) 159–175, https://doi.org/10.1194/jlr.R062885.

[2] Y.H. Tsai, X. Liu, P.H. Seeberger, Chemical Biology of glycosylphosphatidylinositol anchors, Angew. Chem. Int. Ed. 51 (2012) 11438–11456, https://doi.org/10.1002/anie.201203912.

[3] B.Y. Lee, P.H. Seeberger, D. Varon Silva, Synthesis of glycosylphosphatidylinositol (GPI)-anchor glycolipids bearing unsaturated lipids, Chem. Commun. 52 (2016) 1586–1589, https://doi.org/10.1039/c5cc07694c.

[4] S.D. Sharma, J. Mullenax, F.G. Araujo, H.A. Erlich, J.S. Remington, Western Blot analysis of the antigens of Toxoplasma gondii recognized by human IgM and IgG antibodies, J. Immunol. 131 (1983) 977–983 http://www.ncbi.nlm.nih.gov/pubmed/6863940 , Accessed date: 20 December 2019.

[5] N. Azzouz, H. Shams-Eldin, S. Niehus, F. Debierre-Grockiego, U. Bieker, J. Schmidt, C. Mercier, M.F. Delauw, J.F. Dubremetz, T.K. Smith, R.T. Schwarz, Toxoplasma gondii grown in human cells uses GalNAc-containing glycosylphosphatidylinositol precursors to anchor surface antigens while the immunogenic Glc-GalNAc-containing precursors remain free at the parasite cell surface, Int. J. Biochem. Cell Biol. 38 (2006) 1914–1925, https://doi.org/10.1016/j.biocel.2006.05.006.

[6] M. Garg, D. Stern, U. Groß, P.H. Seeberger, F. Seeber, D. Varón Silva, Detection of anti- toxoplasma gondii antibodies in human sera using synthetic glycosylphosphatidylinositol glycans on a bead-based multiplex assay, Anal. Chem. 91 (2019) 11215–11222, https://doi.org/10.1021/acs.analchem.9b02154.

[7] S. Götze, N. Azzouz, Y.H. Tsai, U. Groß, A. Reinhardt, C. Anish, P.H. Seeberger, D.V. Silva, Diagnosis of toxoplasmosis using a synthetic glycosylphosphatidyl-inositol glycan, Angew. Chem. Int. Ed. 53 (2014) 13701–13705, https://doi.org/10.1002/anie.201406706.

[8] D. Jain, D.M. Salunke, Antibody specificity and promiscuity, Biochem. J. 476 (2019) 433–447, https://doi.org/10.1042/BCJ20180670.

[9] C.A. Janeway, P.J. Travers, M. Walport, M.J. Shlomchik, Antigen Recognition by B-Cell and T-Cell Receptors, Immunobiology, 2001, https://www.ncbi.nlm.nih.gov/books/NBK10757/ , Accessed date: 9 September 2019.

[10] V.I. Butvilovskaya, S.B. Popleteaeva, V.R. Chechetkin, Z.I. Zubtsova, M.V. Tsybulskaya, L.O. Samokhina, L.I. Vinnitskii, A.A. Ragimov, E.I.I. Pozharitskaya, G.A. Grigoréva, N.Y. Meshalkina, S.V. Golysheva, N.V. Shilova, N.V. Bovin, A.S. Zasedatelev, A.Y. Rubina, Multiplex determination of serological signatures in the sera of colorectal cancer patients using hydrogel biochips, Cancer Med 5 (2016) 1361–1372, https://doi.org/10.1002/cam4.692.

[11] S. Fitzgerald, J.A. O'Reilly, E. Wilson, A. Joyce, R. Farrell, D. Kenny, E.W. Kay, J. Fitzgerald, B. Byrne, G.S. Kijanka, R. O'Kennedy, Measurement of the IgM and IgG autoantibody immune responses in human serum has high predictive value for the presence of colorectal cancer, Clin. Colorectal Canc. 18 (2019), https://doi.org/10.1016/j.clcc.2018.09.009 e53–e60.

[12] A.A. Tikhonov, E.N. Savvateeva, M.A. Chernichenko, V. V Maslennikov, D. V Sidorov, A.Y. Rubina, N.E. Kushlinskii, Analysis of anti-glycan IgG and IgM antibodies in colorectal cancer, Bull. Exp. Biol. Med. 166 (2019) 489–493, https://doi.org/10.1007/s10517-019-04379-2.

[13] J. Wang, D. Lin, H. Peng, Y. Huang, J. Huang, J. Gu, Cancer-derived immunoglobulin G promotes tumor cell growth and proliferation through inducing production of reactive oxygen species, Cell Death Dis. 4 (2013) e945, https://doi.org/10.1038/cddis.2013.474.

[14] P. Zaenker, E.S. Gray, M.R. Ziman, Autoantibody production in cancer-the humoral immune response toward autologous antigens in cancer patients, Autoimmun. Rev. 15 (2016) 477–483, https://doi.org/10.1016/j.autrev.2016.01.017.

[15] H. Zola, A.P. Mohandas, D. Krumbiegel, Monoclonal antibodies: diagnostic uses, ELS, John Wiley & Sons, Ltd, Chichester, UK, 2013, , https://doi.org/10.1002/9780470015902.a0002177.pub3.

[16] N. Wellinghausen, M. Abele-Horn, O.D. Mantke, M. Enders, V. Fingerle, B. Gärtner, J. Hagedorn, H.F. Rabenau, I. Reiter-Owona, K. Tintelnot, M. Weig, H. Zeichhardt, K.-P. Hunfeld, Immunological Methods for the Detection of Infectious Diseases, (2017) https://www.instand-ev.de/fileadmin/uploads/Wissenschaftliche_Aktivitaeten/INSTAND_Schriftenreihe_Band_I_MiQ_Serologie_2018_en.pdf , Accessed date: 15 September 2019.

[17] O. Villard, B. Cimon, C. L'Ollivier, H. Fricker-Hidalgo, N. Godineau, S. Houze, L. Paris, H. Pelloux, I. Villena, E. Candolfi, Serological diagnosis of toxoplasma gondii infection. Recommendations from the French national reference center for toxoplasmosis, Diagn. Microbiol. Infect. Dis. 84 (2016) 22–33, https://doi.org/10.1016/j.diagmicrobio.2015.09.009.

[18] Q. Liu, Z.D. Wang, S.Y. Huang, X.Q. Zhu, Diagnosis of toxoplasmosis and typing of Toxoplasma gondii, Parasites Vectors 8 (2015), https://doi.org/10.1186/s13071-015-0902-6.

[19] I. Aly, E.E. Taher, G. EL nain, H. EL Sayed, F.A. Mohammed, R.S. Hamad, E.M. Bayoumy, Advantages of bioconjugated silica-coated nanoparticles as an innovative diagnosis for human toxoplasmosis, Acta Trop. 177 (2018) 19–24, https://doi.org/10.1016/j.actatropica.2017.09.024.

[20] A. Ahmed, J.V. Rushworth, N.A. Hirst, P.A. Millner, Biosensors for whole-cell bacterial detection, Clin. Microbiol. Rev. 27 (2014) 631–646, https://doi.org/10.1128/CMR.00120-13.

[21] J. Weile, C. Knabbe, Current applications and future trends of molecular diagnostics in clinical bacteriology, Anal. Bioanal. Chem. 394 (2009) 731–742, https://doi.org/10.1007/s00216-009-2779-8.

[22] A. Hushegyi, J. Tkac, Are glycan biosensors an alternative to glycan microarrays ? Anal. Methods Adv. Methods Appl. 6 (2016) 6610–6620, https://doi.org/10.1039/C4AY00692E.

[23] S. Bahrami, A.R. Abbasi, M. Roushani, Z. Derikvand, A. Azadbakht, An electrochemical dopamine aptasensor incorporating silver nanoparticle, functionalized carbon nanotubes and graphene oxide for signal amplification, Talanta 159 (2016) 307–316, https://doi.org/10.1016/j.talanta.2016.05.060.

[24] J.H. Kim, C.H. Cho, M.Y. Ryu, J.-G. Kim, S.-J. Lee, T.J. Park, J.P. Park, Development of peptide biosensor for the detection of dengue fever biomarker, nonstructural 1, PloS One 14 (2019) e0222144, , https://doi.org/10.1371/journal.pone.0222144.

[25] J. Orozco, L.K. Medlin, Electrochemical performance of a DNA-based sensor device for detecting toxic algae, Sensor. Actuator. B Chem. 153 (2011) 71–77, https://doi.org/10.1016/j.snb.2010.10.016.

[26] G. Vásquez, A. Rey, C. Rivera, C. Iregui, J. Orozco, Amperometric biosensor based on a single antibody of dual function for rapid detection of Streptococcus agalactiae, Biosens. Bioelectron. 87 (2017) 453–458, https://doi.org/10.1016/j.bios.2016.08.082.

[27] E.B. Bahadir, M.K. Sezgintürk, A review on impedimetric biosensors, Artif. Cells, Nanomedicine Biotechnol 44 (2016) 248–262, https://doi.org/10.3109/21691401.2014.942456.
[28] S. Johnson, T.F. Krauss, Label-free affinity biosensor arrays: novel technology for molecular diagnostics, Expet Rev. Med. Dev. 14 (2017) 177–179, https://doi.org/10.1080/17434440.2017.1283982.
[29] T. Bertok, L. Lorencova, E. Chocholova, E. Jane, A. Vikartovska, P. Kasak, J. Tkac, Electrochemical impedance spectroscopy based biosensors: mechanistic principles, analytical examples and challenges towards commercialization for assays of protein cancer biomarkers, ChemElectroChem 6 (2019) 989–1003, https://doi.org/10.1002/celc.201800848.
[30] J.D. Schrattenecker, R. Heer, E. Melnik, T. Maier, G. Fafilek, R. Hainberger, Hexaammineruthenium (II)/(III) as alternative redox-probe to Hexacyanoferrat (II)/(III) for stable impedimetric biosensing with gold electrodes, Biosens. Bioelectron. 127 (2019) 25–30, https://doi.org/10.1016/j.bios.2018.12.007.
[31] Y.H. Tsai, S. Götze, N. Azzouz, H.S. Hahm, P.H. Seeberger, D. Varon Silva, A general method for synthesis of GPI anchors illustrated by the total synthesis of the low-molecular-weight Antigen from toxoplasma gondii, Angew. Chem. Int. Ed. 50 (2011) 9961–9964, https://doi.org/10.1002/anie.201103483.
[32] Y.H. Tsai, S. Götze, I. Vilotijevic, M. Grube, D.V. Silva, P.H. Seeberger, A general and convergent synthesis of diverse glycosylphosphatidylinositol glycolipids, Chem. Sci. 4 (2013) 468–481, https://doi.org/10.1039/c2sc21515b.
[33] J. Orozco, C. Jiménez-Jorquera, C. Fernández-Sánchez, Gold nanoparticle-modified ultramicroelectrode arrays for biosensing: a comparative assessment, Bioelectrochemistry 75 (2009) 176–181, https://doi.org/10.1016/j.bioelechem.2009.03.013.
[34] S. Trasatti, O. Petrii, Real surface area measurements in electrochemistry, Pure Appl. Chem. 63 (1991) 711–734, https://doi.org/10.1351/pac199163050711.
[35] A. García-Miranda Ferrari, C. Foster, P. Kelly, D. Brownson, C. Banks, Determination of the electrochemical area of screen-printed electrochemical sensing platforms, Biosensors 8 (2018) 53, https://doi.org/10.3390/bios8020053.
[36] G. Sucilathangam, N. Palaniappan, C. Sreekumar, T. Anna, IgG - Indirect fluorescent antibody technique to detect seroprevalence of Toxoplasma gondii in immunocompetent and immunodeficient patients in southern districts of Tamil Nadu, Indian J. Med. Microbiol. 28 (2010) 354, https://doi.org/10.4103/0255-0857.71835.
[37] S.J. Park, J. Lee, Y. Qi, N.R. Kern, H.S. Lee, S. Jo, I. Joung, K. Joo, J. Lee, W. Im, CHARMM-GUI Glycan Modeler for modeling and simulation of carbohydrates and glycoconjugates, Glycobiology 29 (2019) 320–331, https://doi.org/10.1093/glycob/cwz003.
[38] P. Banerjee, M. Wehle, R. Lipowsky, M. Santer, A molecular dynamics model for glycosylphosphatidyl-inositol anchors: “flop down” or “lollipop”? Phys. Chem. Chem. Phys. 20 (2018) 29314–29324, https://doi.org/10.1039/c8cp04059a.
[39] M. Wehle, I. Vilotijevic, R. Lipowsky, P.H. Seeberger, D. Varon Silva, M. Santer, Mechanical compressibility of the glycosylphosphatidylinositol (GPI) anchor backbone governed by independent glycosidic linkages, J. Am. Chem. Soc. 134 (2012), https://doi.org/10.1021/ja302803r 18964–18972.
[40] O.A. Loaiza, P.J. Lamas-Ardisana, E. Jubete, E. Ochoteco, I. Loinaz, G. Cabañero, I. García, S. Penadés, Nanostructured disposable impedimetric sensors as tools for specific biomolecular interactions: sensitive recognition of concanavalin A, Anal. Chem. 83 (2011) 2987–2995, https://doi.org/10.1021/ac103108m.
[41] A. Shrivastava, V. Gupta, Methods for the determination of limit of detection and limit of quantitation of the analytical methods, Chronicles Young Sci. 2 (2011) 21, https://doi.org/10.4103/2229-5186.79345.
[42] T. Kinoshita, M. Fujita, Y. Maeda, Biosynthesis, remodelling and functions of mammalian GPI-anchored proteins: recent progress, J. Biochem. 144 (2008) 287–294, https://doi.org/10.1093/jb/mvn090.
[43] B. Striepen, C.F. Zinecker, J.B.L. Damm, P.A.T. Melgers, G.J. Gerwig, M. Koolen, J.F.G. Vliegenthart, J.F. Dubremetz, R.T. Schwarz, Molecular structure of the “low molecular weight antigen” of Toxoplasma gondii: a glucose α1-4 N-acetylgalactosamine makes free glycosyl-phosphatidylinositols highly immunogenic, J. Mol. Biol. 266 (1997) 797–813, https://doi.org/10.1006/jmbi.1996.0806.
[44] S. Götze, A. Reinhardt, A. Geissner, N. Azzouz, Y.H. Tsai, R. Kurucz, D.V. Silva, P.H. Seeberger, Investigation of the protective properties of glycosylphosphatidylinositol-based vaccine candidates in a Toxoplasma gondii mouse challenge model, Glycobiology 25 (2015) 984–991, https://doi.org/10.1093/glycob/cwv040.
[45] Y.U. Kwon, R.L. Soucy, D.A. Snyder, P.H. Seeberger, Assembly of a series of malarial glycosylphosphatidylinositol anchor oligosaccharides, Chem. Eur J. 11 (2005) 2493–2504, https://doi.org/10.1002/chem.200400934.
[46] J.C. Hoogvliet, M. Dijksma, B. Kamp, W.P. Van Bennekom, Electrochemical pretreatment of polycrystalline gold electrodes to produce a reproducible surface roughness for self-assembly: a study in phosphate buffer pH 7.4, Anal. Chem. 72 (2000), https://doi.org/10.1021/ac991215y 2016–2021.
[47] M.A. Quiroz, U. Morales, Y. Meas, L. Salgado, Estimación de parámetros de superficie para electrodos de Au policristalino por depósito de Cu a subpotencial, Rev. Mexic. Fisica 5 (1993) 722–737.
[48] S.P. Zankowski, P.M. Vereecken, Electrochemical determination of porosity and surface area of thin films of interconnected nickel nanowires, J. Electrochem. Soc. 166 (2019) D227–D235, https://doi.org/10.1149/2.0311906jes.
[49] A.N. Sekretaryova, M.Y. Vagin, A.V. Volkov, I.V. Zozoulenko, M. Eriksson, Evaluation of the electrochemically active surface area of microelectrodes by capacitive and faradaic currents, ChemElectroChem 6 (2019) 4411–4417, https://doi.org/10.1002/celc.201900989.
[50] P. Córdoba-Torres, T.J. Mesquita, R.P. Nogueira, Relationship between the origin of constant-phase element behavior in electrochemical impedance spectroscopy and electrode surface structure, J. Phys. Chem. C 119 (2015) 4136–4147, https://doi.org/10.1021/jp512063f.
[51] D. Soto, M. Alzate, J. Gallego, J. Orozco, Electroanalysis of an Iron@Graphene-carbon nanotube hybrid material, Electroanalysis 30 (2018) 1521–1528, https://doi.org/10.1002/elan.201800115.
[52] J. Wan, J. Ai, Y. Zhang, X. Geng, Q. Gao, Z. Cheng, Signal-off impedimetric immunosensor for the detection of Escherichia coli O157:H7, Sci. Rep. 6 (2016) 2–7, https://doi.org/10.1038/srep19806.
[53] C.-H. Lin, M.-J. Lin, C.-C. Wu, Effect of the Chain length of a modified layer and surface roughness of an electrode on impedimetric immunosensors, Anal. Sci. 33 (2017) 327–333, https://doi.org/10.2116/analsci.33.327.
[54] D. Du, X. Ye, J. Cai, J. Liu, A. Zhang, Acetylcholinesterase biosensor design based on carbon nanotube-encapsulated polypyrrole and polyaniline copolymer for amperometric detection of organophosphates, Biosens. Bioelectron. 25 (2010) 2503–2508, https://doi.org/10.1016/j.bios.2010.04.018.
[55] P.A. Jenum, B. Stray-Pedersen, A.G. Gundersen, Improved diagnosis of primary Toxoplasma gondii infection in early pregnancy by determination of anti-toxoplasma immunoglobulin G avidity, J. Clin. Microbiol. 35 (1997) 1972–1977, https://doi.org/10.1128/jcm.35.8.1972-1977.1997.
[56] P. Thangarajah, K. Hajissa, W.K. Wong, M.A. Abdullah, N. Ismail, Z. Mohamed, Usefulness of paired samples for the Serodiagnosis of toxoplasmosis infection in a tertiary teaching Hospital in Malaysia, BMC Infect. Dis. 19 (2019) 202, https://doi.org/10.1186/s12879-019-3830-9.
[57] B.J.M. Zegers, J.W. Stoop, E. Reerink-Brongers, P.C. Sander, R.C. Aalberse, R. Ballieux, Serum immunoglobulins in healthy children and adults levels of the five classes, expressed in international units per millilitre, Clin. Chim. Acta 65 (1975) 319–329, https://doi.org/10.1016/0009-8981(75)90257-0.
[58] S. Chen, M.H. Shamsi, Biosensors-on-chip: a topical review, J. Micromech. Microeng. 27 (2017) 083001, , https://doi.org/10.1088/1361-6439/aa7117.
[59] M.I. Prodromidis, A. Economou, New trends in antibody-based electrochemical biosensors, first ed. first ed., in: I. Palchetti, P.-D. Hansen, D. Barcelo (Eds.), Compr. Anal. Chem. Past, Present Futur. Challenges Biosens. Bioanal. Tools Anal. Chem. A Tribut. To Profr. Marco Mascini, vol. 77, Elsevier Ltd, 2017, pp. 237–286, , https://doi.org/10.1016/bs.coac.2017.05.001.
[60] P. Martinkova, A. Kostelnik, T. Valek, M. Pohanka, Main streams in the construction of biosensors and their applications, Int. J. Electrochem. Sci. 12 (2017) 7386–7403, https://doi.org/10.20964/2017.08.02.
[61] L. Kluková, T. Bertok, P. Kasák, J. Tkac, Nanoscale-controlled architecture for the development of ultrasensitive lectin biosensors applicable in glycomics, Anal. Methods. 6 (2014) 4922–4931, https://doi.org/10.1039/c4ay00495g.
[62] C.T. França, C.S.N. Li Wai Suen, A. Carmagnac, E. Lin, B. Kiniboro, P. Siba, L. Schofield, I. Mueller, IgG antibodies to synthetic GPI are biomarkers of immune-status to both Plasmodium falciparum and Plasmodium vivax malaria in young children, Malar. J. 16 (2017) 1–10, https://doi.org/10.1186/s12936-017-2042-2.
[63] D.O. Procópio, I.C. Almeida, A.C.T. Torrecilhas, J.E. Cardoso, L. Teyton, L.R. Travassos, A. Bendelac, R.T. Gazzinelli, Glycosylphosphatidylinositol-anchored mucin-like glycoproteins from trypanosoma cruzi bind to CD1d but do not elicit dominant innate or adaptive immune responses via the CD1d/NKT cell pathway, J. Immunol. 169 (2002) 3926–3933, https://doi.org/10.4049/jimmunol.169.7.3926.
[64] A. Calderaro, G. Piccolo, S. Peruzzi, C. Gorrini, C. Chezzi, G. Dettori, Evaluation of Toxoplasma gondii immunoglobulin G (IgG) and IgM assays incorporating the new Vidia analyzer system, Clin. Vaccine Immunol. 15 (2008) 1076–1079, https://doi.org/10.1128/CVI.00025-08.
[65] J.A. Goode, J.V.H. Rushworth, P.A. Millner, Biosensor regeneration: a review of common techniques and outcomes, Langmuir 31 (2015) 6267–6276, https://doi.org/10.1021/la503533g.